

Kernel Truncated Regression Representation for Robust Subspace Clustering

Liangli Zhen, Dezhong Peng, Xin Yao

Abstract—Subspace clustering aims to group data points into multiple clusters of which each corresponds to one subspace. Most existing subspace clustering methods assume that the data could be linearly represented with each other in the input space. In practice, however, this assumption is hard to be satisfied. To achieve nonlinear subspace clustering, we propose a novel method which consists of the following three steps: 1) projecting the data into a hidden space in which the data can be linearly reconstructed from each other; 2) calculating the globally linear reconstruction coefficients in the kernel space; 3) truncating the trivial coefficients to achieve robustness and block-diagonality, and then achieving clustering by solving a graph Laplacian problem. Our method has the advantages of a closed-form solution and capacity of clustering data points that lie in nonlinear subspaces. The first advantage makes our method efficient in handling large-scale data sets, and the second one enables the proposed method to address the nonlinear subspace clustering challenge. Extensive experiments on five real-world datasets demonstrate the effectiveness and the efficiency of the proposed method in comparison with ten state-of-the-art approaches regarding four evaluation metrics.

Index Terms—Kernel truncated regression; nonlinear subspace clustering; spectral clustering; kernel techniques.

I. INTRODUCTION

Subspace clustering is one of the most popular techniques for data analysis, which has attracted increasing interests from numerous areas, such as computer vision, image analysis, and signal processing [1]. With the assumption of high-dimensional data lying in a union of low-dimensional subspaces, subspace clustering aims to seek a set of subspaces to fit a given data set and perform clustering based on the identified subspaces.

During past decades, many subspace clustering methods have been proposed, which can be roughly classified into four categories: 1) iterative approaches [2]; 2) statistical approaches [3, 4]; 3) algebraic approaches [5–7]; and 4) spectral clustering-based approaches [8–20]. In recent years, spectral clustering-based approaches have achieved the state-of-the-art in subspace clustering, of which the key is finding a block-diagonal affinity matrix, where the element of the matrix denotes the similarity between two data points and the block-

Liangli Zhen is with the Machine Intelligence Laboratory, College of Computer Science, Sichuan University, Chengdu 610065, China, and the CERCIA, School of Computer Science, University of Birmingham, Birmingham B15 2TT, UK. (e-mail: llzhen@outlook.com).

Dezhong Peng is with the Machine Intelligence Laboratory, College of Computer Science, Sichuan University, Chengdu 610065, China. (pengdz@scu.edu.cn).

Xin Yao is with the CERCIA, School of Computer Science, University of Birmingham, Birmingham B15 2TT, UK. (e-mail: x.yao@cs.bham.ac.uk).

diagonal structure means that only the similarity among intra-cluster data points is nonzero.

To obtain a block-diagonal affinity matrix, most recent spectral clustering-based approaches measure the similarity using so-called self-expression, i.e. representing each data point as a linear combination of the whole data set and then using the representation coefficients to build the affinity matrix. The major difference of those methods is the constraints enforced on the representation coefficients. For example, sparse subspace clustering (SSC) [11] assumes that each data point can be linearly represented by a few of other points. To achieve this end, SSC adopts the ℓ_1 -norm constraint. Low-rank representation (LRR) [12] encourages the coefficient matrix to be low rank, such that it can capture the global structures of data. To obtain low rankness, LRR enforces the nuclear-norm constraint on the coefficients. Different from SSC and LRR, truncated regression representation (TRR) [17, 19] takes Frobenius norm instead of ℓ_1 - and nuclear-norm, which has shown promising performance in many real-world applications. Like most existing subspace clustering algorithms [11–13, 21], the major disadvantage of TRR is that it may not give a satisfactory clustering result when data points cannot be linearly represented with each other. In fact, many real-world data are sampled from multiple nonlinear subspaces, which brings challenges towards TRR and limits its applications in practice.

To group the data drawn from multiple nonlinear subspaces, in this paper, we propose a novel nonlinear subspace clustering method, termed kernel truncated regression representation (KTRR). Our basic idea is based on the following assumption, i.e. there exists a projection space in which the data can be linearly represented. To illustrate this simple but effective idea, we give a toy example in Fig. 1. The proposed method consists of the following steps: 1) projecting the input into another space via an implicit nonlinear transformation; 2) calculating the global self-expression of the whole data set in the projection space in which the data can be linearly reconstructed; 3) eliminating the effect of errors such as Gaussian noise by zeroing trivial coefficients; 4) constructing a Laplacian graph using the obtained coefficients; 5) solving a generalized Eigen-decomposition problem and obtain clustering with k-means. The contributions and novelty of this work could be summarized as follows:

- We propose a novel method which can cluster the data points drawn from multiple nonlinear subspaces. To the best of our knowledge, this is the first nonlinear extension of TRR and one of the first several nonlinear clustering approaches.

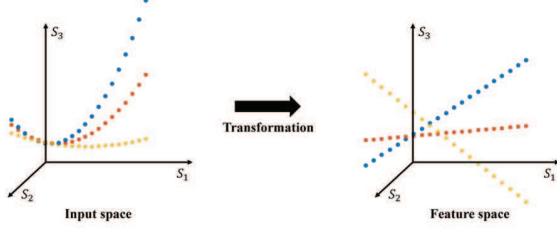


Fig. 1. The basic idea of our method. By projecting the data into another space with an implicit nonlinear transformation, our method could solve the problem of nonlinear subspace clustering. The left and right plots correspond to the distribution of data in the input and hidden space, respectively.

- We develop a closed-form solution to our method. This makes our method very efficient, and useful for large-scale data sets.
- Different from most existing subspace clustering methods like SSC and LRR, KTRR achieves robustness by eliminating the impact of noises in the projection space instead of input space. In other words, KTRR does not require the prior on the structure of errors, which is more competitive to handle corrupted subspaces. Extensive experimental results show that our method significantly outperforms ten other state-of-the-art subspace clustering algorithms regarding accuracy, robustness, and computational cost.

The rest of this paper is organized as follows. Section II discusses some related work. Section III presents the kernel truncated regression and the new robust subspace clustering method. Section IV provides experimental results to illustrate the effectiveness and the efficiency of the proposed algorithm. Section V concludes the paper.

Notations: In this paper, unless specified otherwise, **lower-case bold letters** represent column vectors, **upper-case bold letters** represent matrices, and the entries of matrices are denoted with subscripts. For instance, \mathbf{v} is a column vector, v_i is its i th entry. \mathbf{M} is a matrix, M_{ij} is the entry in the i th row, j th column, and \mathbf{m}_j denotes the j th column of \mathbf{M} . Moreover, \mathbf{M}^T represents the transpose of \mathbf{M} , \mathbf{M}^{-1} denotes the inverse matrix of \mathbf{M} , and \mathbf{I} stands for the identity matrix. Table I summarizes some notations used throughout the paper.

TABLE I
SOME NOTATIONS USED IN THIS PAPER.

Notation	Definition
m	the dimension of input data points
n	the number of input data points
L	the number of underlying subspaces
λ	the balance parameter
$\mathbf{x}_i \in \mathbb{R}^m$	the i th data point
$\mathbf{X} \in \mathbb{R}^{m \times n}$	the data matrix
$\mathbf{X}_i \in \mathbb{R}^{m \times n}$	the dictionary matrix for the data point \mathbf{x}_i
$\mathbf{K} \in \mathbb{R}^{n \times n}$	the kernel matrix of the input data points
$\mathbf{c}_i \in \mathbb{R}^n$	the representation vector for the mapped data point $\phi(\mathbf{x}_i)$
$\mathbf{C} \in \mathbb{R}^{n \times n}$	the linear representation coefficients matrix
$\mathbf{W} \in \mathbb{R}^{n \times n}$	the similarity matrix among all data points
$\mathbf{L} \in \mathbb{R}^{n \times n}$	the normalized Laplacian matrix
$\phi: \mathbb{R}^m \rightarrow \mathcal{H}$	the mapping from the input space to the kernel space
$\kappa(\mathbf{x}_i, \mathbf{x}_j)$	the kernel function

II. RELATED WORK

During past decades, some spectral clustering-based methods have been proposed to achieve subspace clustering in many applications such as image clustering [21], motion segmentation [22], and gene expression analysis [23]. The key of these methods is to obtain a block-diagonal similarity matrix of which nonzero elements are only located on the connections of the points from the same subspace. There are two common strategies to compute the similarity matrix, i.e., pairwise distance-based strategy and linear representation-based strategy [16]. Pairwise distance-based strategy computes the similarity between two points according to their pairwise relationship, e.g., the original spectral clustering method adopts the Euclidean distance with Heat Kernel to calculate the similarity, i.e.,

$$s(\mathbf{x}_i, \mathbf{x}_j) = e^{-\frac{\|\mathbf{x}_i - \mathbf{x}_j\|^2}{2\sigma^2}} \quad (1)$$

where $s(\mathbf{x}_i, \mathbf{x}_j)$ denotes the similarity between the data point \mathbf{x}_i and data point \mathbf{x}_j , and the parameter σ controls the width of the neighborhoods.

Alternatively, linear representation-based approaches assume that each data point could be represented as a linear combination of some points from the intra-subspace. Based on this assumption, the linear representation coefficient can be used as a measurement of similarity and has achieved state of the art in subspace clustering [11–13, 15, 19, 24–26] since it encodes the global structure of the whole data set into similarity.

For given a data matrix $\mathbf{X} = [\mathbf{x}_1, \mathbf{x}_2, \dots, \mathbf{x}_n] \in \mathbb{R}^{m \times n}$, these methods linearly represent \mathbf{X} and obtain the coefficient matrix $\mathbf{C} \in \mathbb{R}^{n \times n}$ in a self-expression manner by solving

$$\min \mathcal{R}(\mathbf{C}) \quad \text{s.t.} \quad \mathbf{X} = \mathbf{X}\mathbf{C}, \text{diag}(\mathbf{C}) = \mathbf{0}, \quad (2)$$

where $\text{diag}(\mathbf{C}) = \mathbf{0}$ avoids the trivial solution which uses the data point to represent itself by enforcing the diagonal elements of \mathbf{C} to be zeros. $\mathcal{R}(\mathbf{C})$ denotes the adopted prior structured regularization on \mathbf{C} and the major difference among most existing subspace clustering methods is the choice of $\mathcal{R}(\mathbf{C})$. For example, SSC [11] enforces the sparsity on \mathbf{C} by adopting ℓ_1 -norm via $\mathcal{R}(\mathbf{C}) = \|\mathbf{C}\|_1$, LRR [12] obtains low rankness by using nuclear norm with $\mathcal{R}(\mathbf{C}) = \|\mathbf{C}\|_*$. To further achieving robustness, (2) is extended as follows:

$$\min \mathcal{R}(\mathbf{C}) + \varphi(\mathbf{E}) \quad \text{s.t.} \quad \mathbf{X} = \mathbf{X}\mathbf{C} + \mathbf{E}, \text{diag}(\mathbf{C}) = \mathbf{0}, \quad (3)$$

where \mathbf{E} stands for the errors induced by the noise and corruption, $\varphi(\mathbf{E})$ measures the impact of the errors. Generally, the $\varphi(\cdot) = \|\mathbf{E}\|_F$ and $\varphi(\cdot) = \|\mathbf{E}\|_1$ are used to describe the Gaussian noise and Laplacian noise, respectively. $\|\cdot\|_F$ denotes the Frobenius norm

Due to the assumption on linear reconstruction, those methods failed to achieve nonlinear subspaces clustering. To address this challenging issue, some recent works have been proposed [15, 24], however, the methods have the following two disadvantages: 1) the methods are computationally inefficient since they involve solving ℓ_1 - or nuclear-norm minimization problem; 2) Like SSC and LRR, the methods

need the prior on the errors existed in the data sets to get the correct mathematical formulation. If the prior is inconsistent with the real situation, the methods could achieve inferior performance. To solve these issues, we propose a nonlinear subspace clustering method which is complementary to existing approaches. Noticed that, Peng et al. recently proposed to achieve nonlinearity with deep structures [27, 28], which are first works to leverage deep learning and subspace clustering. However, this has been beyond of the scope of this paper.

III. THE PROPOSED SUBSPACE CLUSTERING METHOD

This section will give the details of our proposed method, which consists of three steps: 1) calculating the kernel truncated regression representation over the whole data set. 2) eliminating the effectiveness of possible errors such as noises from the representation and then building a graph Laplacian. 3) obtaining clustering by performing the k-means algorithm on leading eigenvectors of the graph Laplacian. Moreover, we also give the computational complexity of the proposed method.

A. Kernel Truncated Regression Representation

For a given data set $\{\mathbf{x}_i\}_{i=1}^n$, where $\mathbf{x}_i \in \mathbb{R}^m$, we define a matrix $\mathbf{X} = [\mathbf{x}_1, \mathbf{x}_2, \dots, \mathbf{x}_n]$. Let $\phi: \mathbb{R}^m \rightarrow \mathcal{H}$ be a nonlinear mapping which transforms the input into a kernel space \mathcal{H} , and $\phi(\mathbf{X}_i) = [\phi(\mathbf{x}_1), \dots, \phi(\mathbf{x}_{i-1}), \mathbf{0}, \phi(\mathbf{x}_{i+1}), \dots, \phi(\mathbf{x}_n)]$. After mapping \mathbf{X} into a kernel space, the corresponding $\{\phi(\mathbf{x}_i)\}_{i=1}^n$ is generally believed lying in linear subspaces [15, 24]. Based on this basic idea, we propose to formulate the objective function of our KTRR as follows:

$$\min_{\mathbf{c}_i} \frac{1}{2} \|\phi(\mathbf{x}_i) - \phi(\mathbf{X}_i) \mathbf{c}_i\|_2^2 + \frac{\lambda}{2} \|\mathbf{c}_i\|_2^2, \quad (4)$$

where the first term is the reconstruction error in the kernel space, the second term serves as an ℓ_2 -norm regularization, and λ is a positive real number, which controls the strength of the ℓ_2 -norm regularization term.

For each transformed data representation $\phi(\mathbf{x}_i)$, solving the optimization problem (4), it gives that

$$\mathbf{c}_i = (\phi(\mathbf{X}_i)^T \phi(\mathbf{X}_i) + \lambda \mathbf{I})^{-1} \phi(\mathbf{X}_i)^T \phi(\mathbf{x}_i), \quad (i = 1, \dots, n). \quad (5)$$

Note that it requires $O(n^4 + mn^2)$ for solving the above problems of n data points with dimensionality of m .

To solve (4) more efficiently, we rewrite it as

$$\min_{\mathbf{c}_i} \frac{1}{2} \|\phi(\mathbf{x}_i) - \phi(\mathbf{X}) \mathbf{c}_i\|_2^2 + \frac{\lambda}{2} \|\mathbf{c}_i\|_2^2, \quad \text{s.t.} \quad \mathbf{e}_i^T \mathbf{c}_i = 0, \quad (6)$$

where \mathbf{e}_i is a column vector with all zero elements except the i -th element is 1, and the constraint $\mathbf{e}_i^T \mathbf{c}_i = 0$ eliminates the trivial solution of writing a transformed point as a linear combination of itself.

Using Lagrangian method, we obtain that

$$L(\mathbf{c}_i) = \frac{1}{2} \|\phi(\mathbf{x}_i) - \phi(\mathbf{X}) \mathbf{c}_i\|_2^2 + \frac{\lambda}{2} \|\mathbf{c}_i\|_2^2 + \theta \mathbf{e}_i^T \mathbf{c}_i, \quad (7)$$

where θ is the Lagrangian multiplier. Clearly,

$$\frac{\partial L(\mathbf{c}_i)}{\partial \mathbf{c}_i} = (\phi(\mathbf{X})^T \phi(\mathbf{X}) + \lambda \mathbf{I}) \mathbf{c}_i - \phi(\mathbf{X})^T \phi(\mathbf{x}_i) + \theta \mathbf{e}_i. \quad (8)$$

Let $\frac{\partial L(\mathbf{c}_i)}{\partial \mathbf{c}_i} = 0$, we get

$$\mathbf{c}_i = (\phi(\mathbf{X})^T \phi(\mathbf{X}) + \lambda \mathbf{I})^{-1} (\phi(\mathbf{X})^T \phi(\mathbf{x}_i) - \theta \mathbf{e}_i). \quad (9)$$

Multiplying \mathbf{e}_i on both sides of (9), and since $\mathbf{e}_i^T \mathbf{c}_i = 0$, it holds that

$$\theta = \frac{\mathbf{e}_i^T (\phi(\mathbf{X})^T \phi(\mathbf{X}) + \lambda \mathbf{I})^{-1} \phi(\mathbf{X})^T \phi(\mathbf{x}_i)}{\mathbf{e}_i^T (\phi(\mathbf{X})^T \phi(\mathbf{X}) + \lambda \mathbf{I})^{-1} \mathbf{e}_i}. \quad (10)$$

Substituting (10) into (9), the optimal solution is given as

$$\mathbf{c}_i = \mathbf{q}_i - \mathbf{P} \frac{\mathbf{e}_i^T \mathbf{q}_i \mathbf{e}_i}{\mathbf{e}_i^T \mathbf{P} \mathbf{e}_i}, \quad (11)$$

where $\mathbf{q}_i = \mathbf{P}(\phi(\mathbf{X})^T \phi(\mathbf{x}_i))$, and $\mathbf{P} = (\phi(\mathbf{X})^T \phi(\mathbf{X}) + \lambda \mathbf{I})^{-1}$.

One can find that the solution to (11) does not require $\phi(\mathbf{x}_i)$ to be explicitly computed, i.e. we will only need their dot products. Therefore, we can employ kernel functions for computing these dot products without explicitly performing the mapping ϕ . For some choices of a kernel $\kappa(\mathbf{x}_i, \mathbf{x}_j): \mathbb{R}^m \times \mathbb{R}^m \rightarrow \mathbb{R}$, [29] has shown that κ can get the dot product in the kernel space \mathcal{H} induced by the mapping ϕ .

We can combine all the dot products as a matrix $\mathbf{K} \in \mathbb{R}^{N \times N}$ whose elements are calculated as

$$K_{ij} = \phi(\mathbf{x}_i)^T \phi(\mathbf{x}_j) = [\phi(\mathbf{X})^T \phi(\mathbf{X})]_{ij} = \kappa(\mathbf{x}_i, \mathbf{x}_j), \quad (12)$$

where $\phi(\mathbf{X}) = [\phi(\mathbf{x}_1), \phi(\mathbf{x}_2), \dots, \phi(\mathbf{x}_n)]$. The matrix \mathbf{K} is the kernel matrix, which is a symmetric and positive semidefinite matrix. Accordingly, (11) can be rewritten as

$$\mathbf{c}_i^* = \mathbf{v}_i - \mathbf{U} \frac{\mathbf{e}_i^T \mathbf{v}_i \mathbf{e}_i}{\mathbf{e}_i^T \mathbf{U} \mathbf{e}_i}, \quad (13)$$

where $\mathbf{v}_i = \mathbf{U} \mathbf{k}_i$, and $\mathbf{U} = (\mathbf{K} + \lambda \mathbf{I})^{-1}$.

It is notable that only one pseudo-inverse operation is needed for solving the representation problems of all data points. The computational complexity of calculating the optimal solutions in (13) has decreased to $O(n^3 + mn^2)$ for n data points with m dimensions.

It has been proved that, under certain condition, the coefficients over intra-subspace data points are larger than those over inter-subspace data points [17]. After representing the data set by the kernel matrix via (13), we handle the errors by performing a hard thresholding operator $\mathcal{T}_\eta(\cdot)$ over \mathbf{c}_i , where $\mathcal{T}_\eta(\cdot)$ keeps η largest entries in \mathbf{c}_i and sets other entries as zeros like TRR, i.e.,

$$\mathcal{T}_\eta(\mathbf{c}_i) = [\mathcal{T}_\eta(C_{1i}), \mathcal{T}_\eta(C_{2i}), \dots, \mathcal{T}_\eta(C_{ni})]^T \quad (14)$$

and

$$\mathcal{T}_\eta(C_{ji}) = \begin{cases} C_{ji}, & \text{if } C_{ji} \in \Omega_i; \\ 0, & \text{otherwise,} \end{cases} \quad (15)$$

where Ω_i consists of η largest elements of \mathbf{c}_i . Typically, the optimal η equals to the dimensionality of corresponding kernel

subspace. In this manner, it avoids to model the impact of the noises into the optimization problem explicitly and does not need the prior knowledge about the errors.

B. KTRR for Robust Subspace Clustering

In this section, we present the method to achieve subspace clustering by incorporating the KTRR into spectral clustering framework [8].

For a given data set \mathbf{X} which consists of n data points in \mathbb{R}^m , we assume that these points should be lying in a union of L low-dimensional nonlinear subspaces. We propose to project the data points into another space, in which the mapped points can be linearly represented by these mapped points from the intra-subspace. From (11), we find that the representation coefficients does not require the projection function in explicit form, but are only needed in dot products. We can induce a kernel function to calculate these dot products, and obtain the representation coefficients via (13).

Moreover, the existence of the errors in the input data set leads to some error connections among the data points from different subspaces. We propose to remove these errors through a hard thresholding on each column vector of the coefficient matrix \mathbf{C} via (14).

As we claimed before, these representation coefficients can be seen as the similarities among the input data points. The similarity between two intra-subspace data points is large, and that between two inter-subspace data points is zero or very close to zero. Such that we can build a similarity matrix \mathbf{W} based on the obtained coefficient matrix \mathbf{C} as

$$\mathbf{W} = |\mathbf{C}^T| + |\mathbf{C}|. \quad (16)$$

This is a symmetric similarity matrix which is suitable for integrating into the spectral clustering framework.

Then, we compute the normalized Laplacian matrix [8]

$$\mathbf{L} = \mathbf{I} - \mathbf{D}^{-\frac{1}{2}} \mathbf{W} \mathbf{D}^{-\frac{1}{2}}, \quad (17)$$

where \mathbf{D} is a diagonal matrix with $D_{ii} = \sum_{j=1}^n W_{ij}$. The matrix \mathbf{L} is positive semi-definite and has an eigenvalue equals 0 with eigenvector $\mathbf{D}^{\frac{1}{2}} \mathbf{1}$ [9], where $\mathbf{1} = [1, 1, \dots, 1]^T \in \mathbb{R}^n$.

Next, we calculate the first L eigenvectors $\mathbf{y}_1, \mathbf{y}_2, \dots, \mathbf{y}_L$ of \mathbf{L} , which corresponding to its first L smallest nonzero eigenvalues, and construct a matrix $\mathbf{Y} = [\mathbf{y}_1, \mathbf{y}_2, \dots, \mathbf{y}_L] \in \mathbb{R}^{n \times L}$.

Finally, we apply the k-means clustering method on the matrix \mathbf{Y} , by treating each row vector as a point, to get the clustering membership. The proposed subspace clustering algorithm is summarized in Algorithm 1.

C. Computational Complexity Analysis

Given a data matrix $\mathbf{X} \in \mathbb{R}^{m \times n}$, the KTRR takes $O(mn^2)$ to compute the kernel matrix \mathbf{K} . Then it takes $O(n^3)$ to obtain the matrix \mathbf{U} , and $O(mn^2)$ to calculate all the solutions in (13) with the matrices \mathbf{U} and \mathbf{K} . Finally, it requires $O(\eta \log n)$ to find η largest coefficients in each column of the representation matrix \mathbf{C} . Putting these steps together, we get the computational complexity of KTRR as $O(mn^2 + n^3)$. This computational complexity is the same as that of TRR, and is

Algorithm 1 Learning kernel truncated regression representation for robust subspace clustering

Input: A given data set $\mathbf{X} \in \mathbb{R}^{m \times n}$, the tradeoff parameter λ , thresholding parameter η , and the number of subspaces L .

Output: The clustering labels of the input data points.

- 1: Calculate the kernel matrix \mathbf{K} and the matrix \mathbf{U} in (13) and store them.
- 2: For each point $\mathbf{x}_i \in \mathbb{R}^m$, calculate its linear representation coefficients in the kernel space $\mathbf{c}_i \in \mathbb{R}^n$ via (13).
- 3: Remove the trivial coefficients from \mathbf{c}_i by performing hard thresholding operator $\mathcal{T}_\eta(\mathbf{c}_i)$, i.e., keeping η largest entries in \mathbf{c}_i and zeroing all other elements.
- 4: Construct a symmetric similarity matrix via (16).
- 5: Calculate the normalised Laplacian matrix \mathbf{L} via (17).
- 6: Compute the eigenvector matrix $\mathbf{Y} \in \mathbb{R}^{n \times L}$ that consists of the first L normalized eigenvectors of \mathbf{L} corresponding to its L smallest nonzero eigenvalues.
- 7: Perform k-means clustering algorithm over the rows of \mathbf{Y} to get the clustering membership.

considerably less than that of KSSC ($O(mn^2 + tn^3)$)[30], KLRR($O(t(r_X + r)n^2)$)[24], where t denotes the total number of iterations for the corresponding algorithm, r_X is the rank of \mathbf{X} , and r is the rank for partial SVD at each iteration of KLRR.

IV. EXPERIMENTAL RESULTS AND ANALYSIS

In this section, we experimentally evaluate the performance of the proposed method. We consider the results in terms of three aspects: 1) accuracy, 2) robustness, and 3) computational cost. Robustness is evaluated by conducting experiments using samples with two different types of corruptions, i.e., Gaussian noises and random pixel corruption.

A. Databases

Five popular image databases are used in our experiments, including Extended Yale Database B (ExYaleB) [31], Columbia Object Image Library (COIL 20) [32], Columbia Object Image Library (COIL 100) [33], USPS [34], and MNIST [35]. We give the details of these databases as follows:

- The ExYaleB database contains 2414 frontal face images of 38 subjects and around 64 near frontal images under different illuminations per individual, where each image is manually cropped and normalized to the size of 32×32 pixels [36].
- The COIL 20 and COIL 100 databases contain 20 and 100 objects respectively. The images of each object were taken 5 degrees apart as the object is rotated on a turntable and each object has 72 images. The size of each image is 32×32 pixels, with 256 grey levels per pixel [36].
- The USPS handwritten digit database¹ includes ten classes (0–9 digit characters) and 11000 samples in total.

¹The USPS database and MNIST database used in this paper are download from <http://www.cad.zju.edu.cn/home/dengcai/Data/MLData.html>.

We use a popular subset contains 9298 handwritten digit images for the experiments, and all of these images are normalized to the size of 16×16 pixels. In the experiment, we select 200 samples of each subject from the database randomly by following the strategy in [10].

- The MNIST handwritten digit database includes ten classes (0 – 9 digit characters) and 60000 samples in total. We use first 10000 handwritten digit images of the training subset to conduct the experiments, and all of these images are normalized to the size of 28×28 pixels. In the experiment, we also select 200 samples of each subject from the database randomly to evaluate the performance of different algorithms.

The details of these real-world databases are summarized in Table II

TABLE II

DETAILS OF SEVEN DATA SETS FOR THE EXPERIMENTS. FOR SIMPLICITY, c DENOTES THE TOTAL NUMBER OF CLUSTERS, AND n_i STANDS FOR THE NUMBER OF SAMPLES IN EACH CLUSTER.

Dataset	c	n_i	Original size	Normalised size
ExYaleB	38	58	192×168	32×32
COIL 20	20	72	128×128	32×32
COIL 100	100	72	128×128	32×32
USPS	10	1000	16×16	16×16
MNIST	10	1000	28×28	28×28

B. Baselines and Evaluation Metrics

We compare KTRR² with 10 state-of-art subspace clustering algorithms including truncated regression representation (TRR) [17], kernel low-rank representation (KLRR) [24], kernel sparse subspace clustering (KSSC) [30], Latent low-rank representation (LatLRR) [25], low-rank representation (LRR1) with ℓ_1 -norm [12], low-rank representation (LRR2) with ℓ_{21} -norm [12], sparse subspace clustering (SSC) [11], sparse manifold clustering and embedding (SMCE) [26], local subspace analysis (LSA) [37], and standard spectral clustering (SC) [8].

For a fair comparison, we use the same spectral clustering framework [8] with different similarity matrices obtained by the tested algorithms. Like [24], for all kernel-based algorithms, we adopt the commonly used Gaussian kernel on all datasets and use the default bandwidth parameter which is set to the mean of the distances between all the samples.

Four popular metrics are adopted to evaluate the subspace clustering quality, i.e., accuracy (AC) [10, 38], normalized mutual information (NMI) [10, 38], the adjusted rand index (ARI) [39], and Fscore [40]. The values of above four metrics are higher if the method works better. The values of these four metrics are equal to 1 indicates the predict results is perfectly matching with the ground truth, whereas 0 indicates totally mismatch.

²The source code of our proposed method are available at <https://www.dropbox.com/s/8vj1k1b184w2ksv/KTRR.zip?dl=0>.

C. Visualisation of Representation and Similarity Matrices

Before evaluating the clustering performance of the proposed method, we illustrate the visualization results of the KTRR coefficients matrix and the obtained similarity matrix. We get the result by using the first 128 facial images in the ExYaleB database, first 64 samples of which belong to the first subject, and the other 64 samples belong to the second subject. We set the parameters as $\lambda = 5$, $\eta = 4$. The representation matrix \mathbf{C} in (13) and the constructed similarity matrix \mathbf{W} are shown in Fig. 2(a) and Fig. 2(b) respectively.

From Fig. 2(a), we can see that the upper-left part and the bottom-right part are illuminated from the upper-right part and the bottom-left part, but there still exist some non-zero elements in the upper-right part and the bottom-left part. That is to say, the connections among the same subject are much stronger than that among different subjects, while there are many trivial connections among the samples from different subjects since the samples from various subjects are facial images, which have some common characteristics.

As we know, an ideal similarity matrix for the spectral clustering algorithm is a block diagonal matrix, i.e., the connections should only exist among the data points from the same cluster [12, 15, 17, 24, 26], such that a hard thresholding operation has been executed. From the result of similarity matrix \mathbf{W} in Fig. 2(b), we find that:

- Our method reveals the latent structure of data though these images belong to the two subjects. There exist only a few bright spots in the upper-right part and the bottom-left part of the obtained similarity matrix, i.e., the trivial connections among the samples from different subjects have been mostly removed by using the thresholding processing;
- Almost all of the bright spots lie in the diagonal blocks of the similarity matrix, i.e., the strong connections exist among the samples from the same subject;
- The obtained similarity matrix is a symmetric matrix which can be directly used for subspace clustering under the framework of spectral clustering [8].

D. Clustering on Clean Images

In this experiment, we compare the KTRR method with other ten state-of-the-art approaches on four different benchmark databases, i.e., Extended Yale Database B (ExYaleB) [31], Columbia Object Image Library (COIL 20) [32], USPS [34], MNIST [35]. For each dataset, we perform each algorithm 10 runs, in each run the k-means clustering step are repeated 500 times, and report the mean and the standard deviation of the used metrics. The clustering quality on above four databases are shown in Table III - Table VI. The better means for each database are highlighted in boldface. To have statistically sound conclusions, the Wilcoxon's rank sum test [41] at a 0.05 significance level is adopted to test the significance of the differences between the results obtained by the proposed method and all other algorithms. From the results, we can obtain the following conclusions.

(1) Evaluation on the ExYaleB facial database:

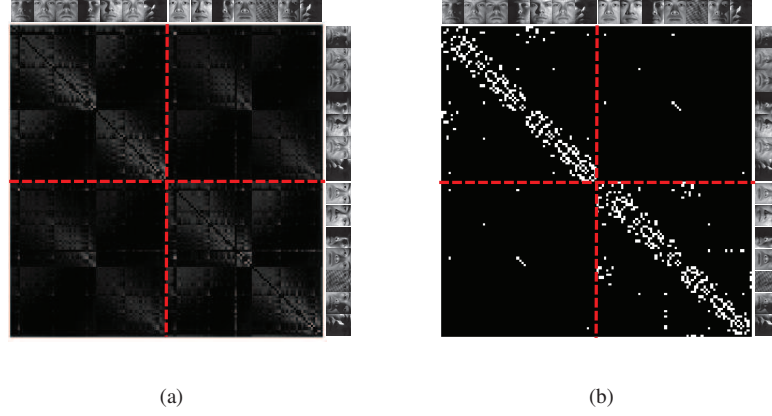


Fig. 2. The visualization of the representation matrix and the similarity matrix on 128 facial images which from first 2 subjects in ExYaleB database. (a) The representation matrix in (13). (b) The similarity matrix obtained by our algorithm. The experiment was carried out on the first two subjects of ExYaleB. The top rows and the right columns illustrate some images of these two subjects. The dotted lines split each matrix into four parts. The upper-left part: the similarity relationship among the 64 images of the first subject. The bottom-right part: the similarity relationship among the 64 images of the second subject. The upper-right part and the bottom-left part: the similarity relationship among the images from different subjects. From the connections, it is easy to find that the upper-left part and the bottom-right part are illuminated from the upper-right part and the bottom-left part, which means that our method reflects the correct relationship among the samples from different subjects.

TABLE III

CLUSTERING PERFORMANCE (%) COMPARISONS IN DIFFERENT METHODS ON THE EXYALEB DATABASE. THE BEST MEAN RESULTS IN DIFFERENT METRICS ARE IN BOLD. THE “†” INDICATES THAT THE VALUE OF THE METHOD IS SIGNIFICANTLY DIFFERENT FROM ALL OTHER METHODS AT A 0.05 LEVEL BY THE WILCOXON’S RANK SUM TEST.

Metric	KTRR	TRR	KLRR	KSSC	LatLRR	LRR1	LRR2	SSC	SMCE	LSA	SC
AC	84.82+5.75[†]	67.04+2.93	52.30+4.31	58.41+3.19	51.40+3.36	50.32+2.68	49.80+4.72	52.87+5.46	48.91+3.71	33.97+3.95	19.69+1.70
NMI	89.52+2.43[†]	72.20+2.61	61.98+2.45	64.41+1.10	54.41+1.76	53.31+1.42	53.26+2.22	58.02+3.44	60.22+1.28	47.38+1.87	32.96+1.54
ARI	77.09+5.84[†]	41.07+6.91	36.06+3.49	32.40+5.82	27.10+2.26	26.42+2.17	25.63+2.70	24.20+4.74	30.46+3.06	20.98+1.45	10.16+1.01
Fscore	77.72+5.66[†]	43.01+6.52	37.87+3.37	34.59+5.38	29.33+2.07	28.66+2.00	27.93+2.52	26.83+4.34	32.54+2.84	23.20+1.36	12.56+0.98

TABLE IV

CLUSTERING PERFORMANCE (%) COMPARISONS IN DIFFERENT METHODS ON THE COIL 20 DATABASE. THE BEST MEAN RESULTS IN DIFFERENT METRICS ARE IN BOLD. THE “†” INDICATES THAT THE VALUE OF THE METHOD IS SIGNIFICANTLY DIFFERENT FROM ALL OTHER METHODS AT A 0.05 LEVEL BY THE WILCOXON’S RANK SUM TEST.

Metric	KTRR	TRR	KLRR	KSSC	LatLRR	LRR1	LRR2	SSC	SMCE	LSA	SC
AC	90.25+6.13[†]	84.12+3.35	68.66+5.51	79.39+8.15	67.97+3.47	67.94+7.97	66.59+3.35	69.39+5.93	76.51+15.98	72.86+6.67	69.17+3.81
NMI	94.71+2.75[†]	91.79+0.94	77.93+3.24	89.50+2.73	76.78+1.32	76.45+2.20	75.33+2.50	80.61+2.44	90.51+5.69	81.49+3.69	79.43+2.18
ARI	88.04+5.49[†]	80.72+3.05	61.96+6.98	76.54+7.13	60.03+2.42	60.03+4.94	58.45+4.21	62.14+5.18	75.20+15.45	68.13+5.92	63.77+3.88
Fscore	88.65+5.19[†]	81.76+2.80	63.92+6.55	77.81+6.65	62.03+2.30	62.09+4.66	60.57+3.98	64.17+4.80	76.61+14.41	69.74+5.57	65.60+3.68

TABLE V

CLUSTERING PERFORMANCE (%) COMPARISONS IN DIFFERENT METHODS ON THE USPS HANDWRITING DATABASE. THE BEST MEAN RESULTS IN DIFFERENT METRICS ARE IN BOLD. THE “†” INDICATES THAT THE VALUE OF THE METHOD IS SIGNIFICANTLY DIFFERENT FROM ALL OTHER METHODS AT A 0.05 LEVEL BY THE WILCOXON’S RANK SUM TEST.

Metric	KTRR	TRR	KLRR	KSSC	LatLRR	LRR1	LRR2	SSC	SMCE	LSA	SC
AC	81.36+14.93[†]	60.24+16.98	70.72+2.63	75.17+2.89	70.97+4.10	70.16+4.29	70.91+3.96	26.86+13.39	73.77+7.85	68.51+8.95	70.79+8.58
NMI	78.04+6.63[†]	59.55+7.61	66.23+3.35	73.97+2.41	66.55+4.37	66.69+4.63	66.87+4.35	20.93+13.44	71.29+9.69	64.80+7.93	62.72+4.55
ARI	71.73+12.67[†]	46.06+13.33	57.21+3.76	65.11+3.67	57.20+4.51	57.18+4.79	57.50+4.48	9.95+13.56	62.08+13.10	55.58+9.00	53.55+5.24
Fscore	74.69+11.13[†]	51.98+11.29	61.64+3.41	68.76+3.28	61.59+4.11	61.58+4.34	61.85+4.08	24.07+7.62	66.10+11.63	60.30+7.99	58.25+4.67

TABLE VI

CLUSTERING PERFORMANCE (%) COMPARISONS IN DIFFERENT METHODS ON THE MNIST HANDWRITING DATABASE. THE BEST MEAN RESULTS IN DIFFERENT METRICS ARE IN BOLD. THE “†” INDICATES THAT THE VALUE OF THE METHOD IS SIGNIFICANTLY DIFFERENT FROM ALL OTHER METHODS AT A 0.05 LEVEL BY THE WILCOXON’S RANK SUM TEST.

Metric	KTRR	TRR	KLRR	KSSC	LatLRR	LRR1	LRR2	SSC	SMCE	LSA	SC
AC	63.97+8.11[†]	32.19+16.22	61.31+6.14	57.13+15.57	14.48+8.37	18.08+10.57	18.52+12.34	22.02+20.53	61.66+5.59	63.03+7.46	55.11+5.45
NMI	66.81+4.43[†]	24.73+15.97	60.07+5.86	59.43+13.06	4.04+7.96	6.76+11.18	7.53+14.97	14.58+24.25	59.08+3.99	61.94+5.78	48.80+5.30
ARI	52.63+5.04[†]	12.35+13.93	47.46+5.77	45.02+16.11	1.26+4.47	2.80+6.50	3.27+8.64	6.16+16.06	46.81+5.80	49.50+8.19	36.95+5.62
Fscore	57.92+4.16[†]	24.31+8.95	52.99+4.92	50.99+14.05	18.13+2.74	18.42+4.13	18.43+5.15	21.67+9.34	52.39+5.05	54.78+7.28	43.38+5.01

- All linear and non-linear representation methods, i.e., KTRR, TRR [17], KLRR [24], KSSC [15], LRR [12], SSC [11], outperform the standard spectral clustering method [8].
- All the linear representation methods, i.e., TRR [17], LRR [12], and SSC [11], are inferior to their kernel-based extensions, i.e., KTRR, KLRR [24], and KSSC [15]. It means that the non-linear representation methods are more suitable to model the ExYaleB facial images.
- The KTRR algorithm achieves the best results in the tests and gains a significant improvement over TRR. The means of *Accuracy*, *NMI*, *ARI*, and *Fscore* of KTRR are about 17%, 17%, 26% and 24% higher than that of the TRR, 32%, 28%, 41%, and 40% higher than that of the KLRR.

(2) Evaluation on the COIL 20 database:

- All the linear representation methods, i.e., TRR [17], LRR [12], and SSC [11], are still inferior to their kernel-based extensions, i.e., KTRR, KLRR [24], and KSSC [15]. Their non-linear versions obtain the *Accuracy* improvements of 6.13%, 0.68%, and 10%, respectively.
- The KTRR algorithm gets the *Accuracy* of 90.25%, which is better than all other tested methods. Specifically, the *Accuracy* of KTRR is about 6.13% higher than that of the second best method TRR, and 21.86% higher than that of the third best method KLRR.
- The KLRR, LatLRR and two types of LRR methods are all inferior to the standard spectral method.

(3) Evaluation on the USPS handwriting database:

- All the linear representation methods, i.e., TRR [17], LRR [12], and SSC [11], are inferior to their kernel-based extensions, i.e., KTRR, KLRR [24], and KSSC [15]. The performance improvement is considerable, e.g., the *Accuracy* of KSSC is about 44% higher than that of SSC.
- SSC is inferior to LRR, while its kernel-based extension KLRR outperforms the kernel-based extension of LRR. The implicit transformation on the USPS images makes the mapped data points to be much better represented with each other in a sparse representation form.
- The KTRR algorithm achieves the best results in the tests. The *Accuracy* of KTRR is about 21% higher than that of the TRR, 10% higher than that of the KLRR, and 6% higher than that of the KSSC. The performance indices of KTRR on *NMI*, *ARI*, and *Fscore* are also greater than other tested methods.

(4) Evaluation on the MNIST handwriting database:

- All the linear representation methods, i.e., TRR [17], LRR [12], and SSC [11], are inferior to their kernel-based extensions, i.e., KTRR, KLRR [24], and KSSC [15]. Especially, LRR results in poor performance on this database, while its kernel-based version, KLRR, obtains much better clustering quality regarding *Accuracy*, *NMI*, *ARI*, and *Fscore*.
- The KTRR, KLRR, SMCE and LSA algorithms achieve the best clustering results on the MNIST handwriting

images compared with other methods. However, the performances of all the test methods are not well.

- The proposed method KTRR achieves the best clustering result and obtains a significant improvement of 31.78% at *Accuracy* on TRR. The indexes *NMI*, *ARI*, and *Fscore* of KTRR are also higher than all other tested methods.

E. Clustering on Corrupted Images

To evaluate the robustness of the proposed method, we conduct the experiments on the first 10 subjects of COIL20 database and ExYaleB database respectively. All used images are corrupted by additive white Gaussian noises or random pixel corruptions. Some corrupted image samples under different levels of noises are as shown in Fig. 3. Actually, for the additional Gaussian noises, we add the noises with *SNR* equals 10, 20, 30, 40, 50 dB; For the random pixel corruptions, we adopt the pepper & salt noises with the ratios of affected pixels be 5%, 10%, 15%, 20%, 25%.

The clustering quality of the compared methods on the two databases with additional Gaussian noises is shown in Fig. 4, from which we can get the following observations:

- Most of these spectral-based methods are relatively robust to the additional Gaussian noises. While the performance of LRR1, LRR2, and LatLRR are sharply deteriorated on these two databases. The main reason may be that the additional Gaussian noises have destroyed the underlie the low-rank structure of the representation matrix.
- The accuracy of all tested methods on COIL20 database are higher than that on ExYaleB database. It is consistent with the result of that on clean images.
- The proposed KTRR is considerably more robust than other methods for additional Gaussian noises. Specifically, KTRR obtains the *Accuracy* around 80% under *SNR* = 10dB, which are much higher than all other tested algorithms, especially SC, LSA, LRR1, and LRR2.

The clustering quality of the compared methods on the images with randomly corruptions is shown in Fig. 5, from which we obtain that:

- All the investigated methods perform not as well as the case with white Gaussian noise. The result is consistent with a widely-accepted conclusion that non-additive corruptions are more challenging than additive ones in pattern recognition;
- All of the test algorithms perform much better on COIL20 database than on ExYaleB database. The *Accuracy* of all algorithms are lower than 40% on ExYaleB under 20% and 25% of corrupted pixels. From the Fig. 3, we find that most pixel values of the images from COIL20 database are close to 0 or 255. This leads to some of the corruptions to be useless and weakens the impact to the final clustering results.
- The KTRR algorithm is robust to the random pixel corruptions. It achieves the best results under the ratio of affected pixels equals 5% to 15% on the test two databases. It obtains the *Accuracy* around 60% under the ratio of affected pixels equals 25% on COIL20 database,



Fig. 3. (a) The corrupted samples with additional Gaussian noises under SNR equals 10, 20, 30, 40, 50 dB from left to right. (b) The corrupted samples with pepper and salt noises under the ratio of affected pixels equals 5%, 10%, 15%, 20%, 25% from left to right.

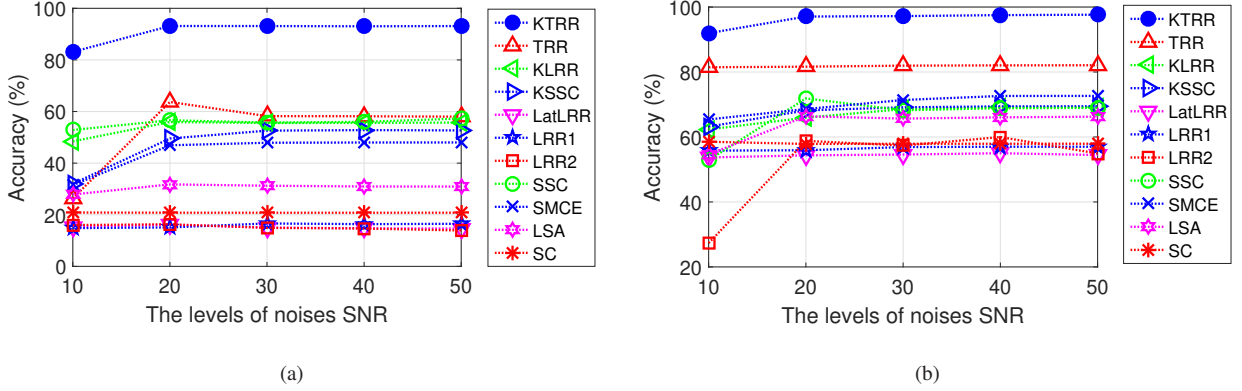


Fig. 4. The clustering results on images with different levels of additional Gaussian noises. (a) The clustering accuracy on the ExYaleB database. (b) The clustering accuracy on the COIL 20 database.

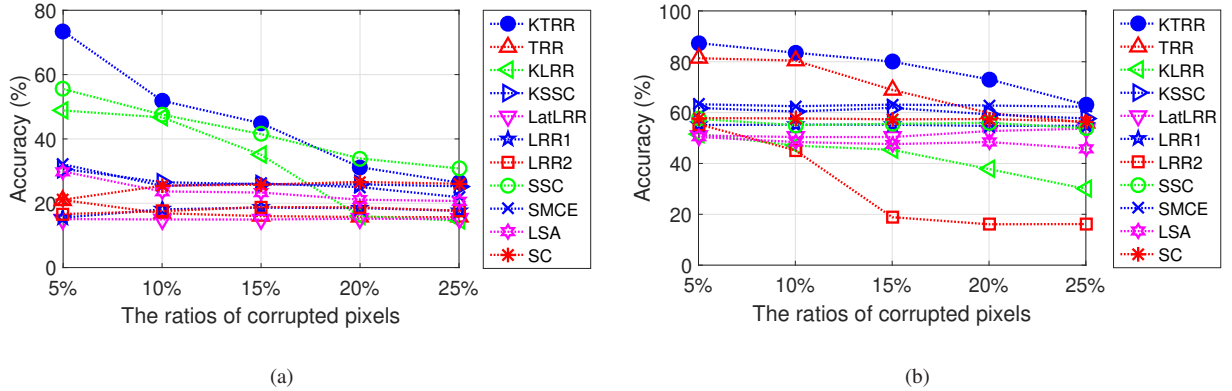


Fig. 5. The clustering results on images with different ratios of pepper & salt corruptions. (a) The clustering accuracy on the ExYaleB database. (b) The clustering accuracy on the COIL 20 database.

which is a very challenging situation that we can see in Fig. 3. However, the *Accuracy* of KTRR drops severely with the increase of the ratios of corrupted pixels, and lower than that of SSC under 20% and 25% of corrupted pixels. The KTRR should be improved to handle the images with salt & pepper corruptions.

F. Computational Time

To investigate the efficiency of KTRR, we compare its computational time with that of other 10 approaches on the clean images of four databases. Our hardware configuration comprises of a 2.4-GHz CPU and a 16 GB RAM. The time cost for building similarity graph (t_1) and the whole time cost

for clustering (t_2) are recorded to evaluate the efficiency of compared methods.

Table VII shows the time cost of different methods with the parameters which achieve their best results. We can see that:

- The standard SC [8] is the fastest since its similarity graph is computing via the pairwise kernel distances among the input samples, while the KSSC [15] is the most time-consuming method.
- The time cost of the proposed method is very close to that of its linear version TRR [17]. Specifically, the TRR method is faster than KTRR on ExYaleB and USPS databases, while it is slower than KTRR on MNIST database. They have similar time cost on COIL database.

TABLE VII

COMPUTATIONAL TIME (SECONDS) COMPARISONS OF DIFFERENT METHODS ON THE EXYALEB, COIL 20, USPS, AND MNIST DATABASES. THE t_1 AND t_2 DENOTE THE TIME COST ON THE SIMILARITY GRAPH CONSTRUCTION PROCESS AND THE TIME COST ON THE WHOLE CLUSTERING PROCESS OF EACH METHOD RESPECTIVELY. THE BEST MEAN RESULTS IN DIFFERENT METRICS ARE IN BOLD.

Databases		KTRR	TRR	KLRR	KSSC	LatLRR	LRR1	LRR2	SSC	SMCE	LSA	SC
ExYaleB	t_1	22.96	23.71	45.82	5512.68	772.44	248.94	270.65	2301.75	10.15	198.48	0.33
	t_2	47.62	48.8	71.26	5543.4	806.43	286.91	311.34	2313.31	45.18	229.26	124.45
COIL 20	t_1	6.50	6.54	16.11	1466.12	579.01	430.23	454.87	121.76	5.76	61.14	0.15
	t_2	11.66	12.75	25.55	1472.07	584.46	436.59	460.07	126.88	10.12	66.01	7.61
USPS	t_1	16.92	11.95	29.41	2752.97	50.05	43.34	49.10	62.25	67.44	108.67	0.14
	t_2	27.82	22.74	39.93	2763.19	58.98	51.88	58.90	98.79	76.50	120.46	11.73
MNIST	t_1	22.56	22.43	34.20	5742.89	246.35	155.70	172.32	112.13	16.78	142.71	1.09
	t_2	33.96	32.35	44.64	5753.42	270.19	167.25	186.82	153.23	25.52	154.64	14.65

The Wilcoxon's rank sum test [41] at a 0.05 significance level shows there is no significant difference between the time costs of the KTRR and TRR on the similarity graph construction and the whole clustering process on the tested four databases.

- The KTRR and TRR [17] algorithms are much faster than KSSC, SSC, KLRR, and LRR methods. The results are consist with the fact that the theorectical computation complexities of KTRR and TRR are much lower than that of KSSC, SSC, KLRR, and LRR methods. The KTRR and TRR [17] algorithms both have analytical solutions, and only one pseudo-inverse operation is required for solving the representation problems of all data points for KTRR and TRR algorithms.

G. Clustering Performance with Varying Number of Subjects

In this subsection, we investigate the clustering performance of the proposed method with a different number of subjects on COIL 100 image database. The experiments are carried out on the first t classes of the database, where t increases from 10 to 100 with an interval of 10. The clustering results are shown in Fig. 6.

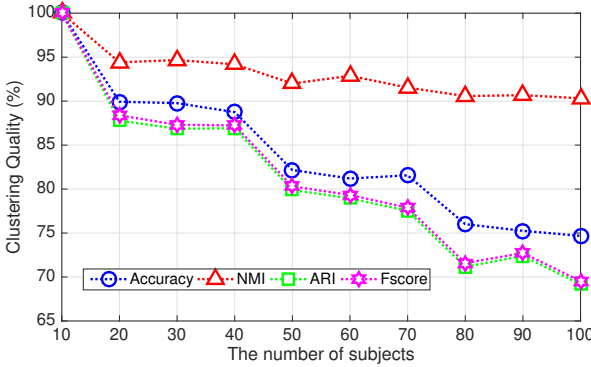


Fig. 6. The clustering quality of the proposed method on the first g subjects of COIL 100 database.

From the results, we can see that:

- In general, with the number of subjects increase, the clustering performance is decreased since the clustering difficulty is increasing with the number of subjects growth.
- With increasing number of subjects, the *NMI* of KTRR is changed slightly, varying from 100% to 90%. The

possible reason is that the *NMI* is robust to the data distribution (increasing subject number) [19].

- The proposed method obtains satisfactory performance on COIL 100 database. It achieves perfect clustering result for $t = 10$, and gets the satisfactory performance at $t = 100$ with *Accuracy*, *NMI*, *ARI*, and *Fscore* be around 74%, 90%, 68%, and 68%, respectively.

H. Parameter Analysis

The KTRR has two parameters, the tradeoff parameter λ and the thresholding parameter η . The selection of the values of the parameters depends on the data distribution. A bigger λ is suitable for highly corrupted databases, and η corresponds to the dimensionality of the corresponding subspace for the mapped data points.

To evaluate the impact of λ and k , we conduct the experiment on the ExYaleB and COIL20 databases. We set the λ from 10^{-5} to 10^2 , and η from 1 to 50, the results are shown in Fig. 7 and Fig. 8 .

From the results, we get the following observations:

- The proposed method achieves the best clustering performance with λ and η as 0.1 and 5 on ExYaleB database, and 10 and 4 on COIL20 database, respectively.
- The proposed method can obtain satisfactory performance with λ from 0.1 to 1 on ExYaleB database, where the *Accuracy*, *NMI*, *ARI*, and *Fscore* are more than 85%, 90%, 75%, and 75%, respectively, and with λ from 0.2 to 100 on COIL20 database, where the *Accuracy*, *NMI*, *ARI*, and *Fscore* are more than 80%, 90%, 80%, and 80%. The performance of KTRR is not sensitive to the parameter of λ , which makes KTRR be suitable for the real applications.
- The clustering quality with η from 3 to 10 on ExYaleB and COIL20 databases are much better than other cases. It means that the thresholding process is helpful to improve the performance of KTRR, and the dimensionality of underlying subspaces of the ExYaleB and COIL20 databases in the hidden space belongs the scope from 3 to 10.

I. Different Kernel Functions

The commonly used kernel functions are polynomial kernels, radial basis functions, and sigmoid kernels. To investigate the performance of the proposed method using different kernels, we study six different kernel functions. The results on

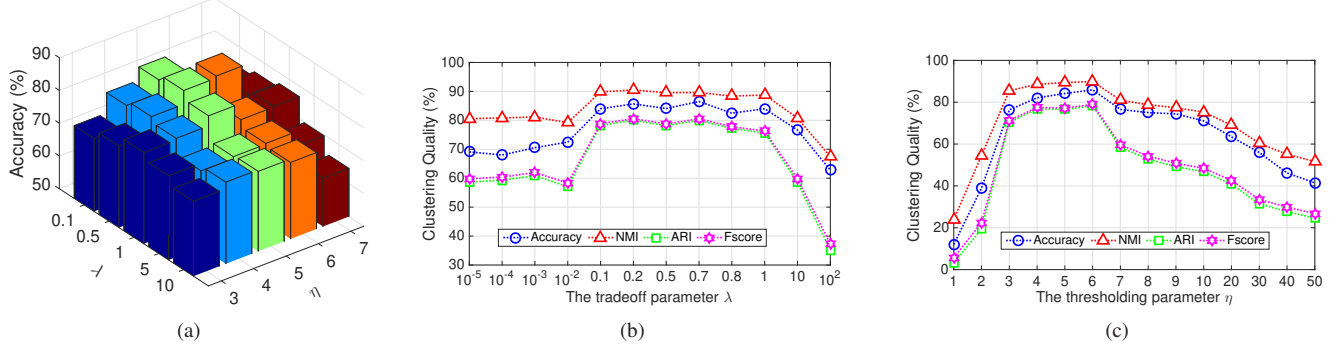


Fig. 7. Clustering performance of the proposed method on ExYaleB database. (a) Clustering performance of the proposed method versus different values of λ and η . (b) Clustering performance of the proposed method versus different values of λ , and fix $\eta = 5$. (c) Clustering performance of the proposed method versus different values of η , and fix $\lambda = 0.5$.

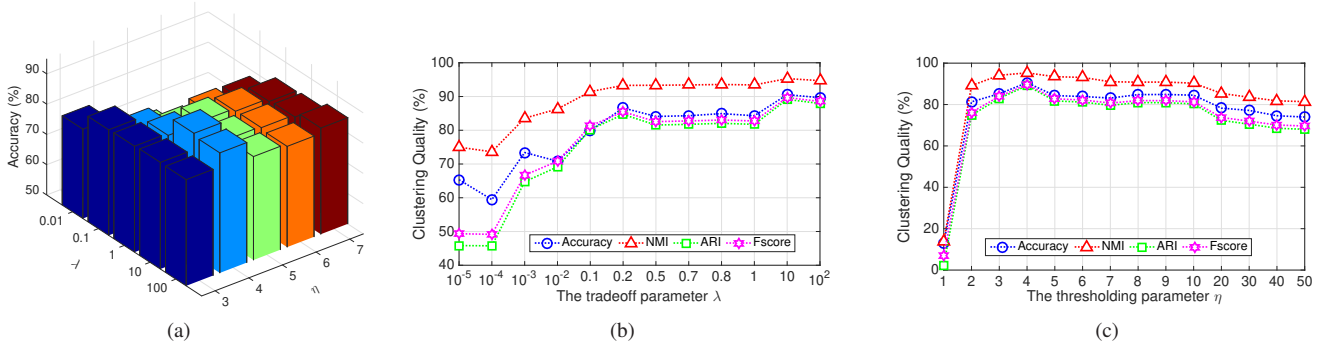


Fig. 8. Clustering performance of the proposed method on COIL20 database. (a) Clustering performance of the proposed method versus different values of λ and η . (b) Clustering performance of the proposed method versus different values of λ , and fix $\eta = 4$. (c) Clustering performance of the proposed method versus different values of η , and fix $\lambda = 10$.

TABLE VIII
PERFORMANCE COMPARISON OF DIFFERENT KERNEL FUNCTIONS USED IN THE PROPOSED METHOD. THE PARAMETER OF σ IS SETTING AS THE MEAN OF THE DISTANCES BETWEEN ALL THE SAMPLES. THE BEST MEAN RESULTS IN DIFFERENT METRICS ARE IN BOLD.

Function $\kappa(\mathbf{x}_i, \mathbf{x}_j)$	$(\mathbf{x}_i^T \mathbf{x}_j)^3$	$(\mathbf{x}_i^T \mathbf{x}_j)^2$	$e^{-\frac{\ \mathbf{x}_i - \mathbf{x}_j\ ^2}{\sigma^2}}$	$e^{-\frac{\ \mathbf{x}_i - \mathbf{x}_j\ }{\sigma}}$	$\frac{1}{\ \mathbf{x}_i - \mathbf{x}_j\ ^2}$	$\frac{1}{\ \mathbf{x}_i - \mathbf{x}_j\ }$
USPS	AC	80.38+19.04	72.31+18.06	81.36+14.93	74.97+12.40	79.62+17.69
	NMI	76.08+9.75	67.38+14.41	78.04+6.63	75.59+9.22	74.18+13.08
	ARI	70.10+15.43	59.48+17.11	71.73+12.67	65.98+13.81	68.32+19.86
	Fscore	73.25+13.45	63.78+15.06	74.69+11.13	69.72+11.83	71.68+17.47
MNIST	AC	65.58+11.65	66.48+14.54	63.97+8.11	59.21+14.27	61.62+12.43
	NMI	64.27+6.25	63.49+6.50	66.81+4.43	63.54+12.66	64.00+9.32
	ARI	51.62+10.21	51.54+11.54	52.63+5.04	48.62+16.10	50.18+11.25
	Fscore	56.70+8.92	56.61+10.09	57.92+4.16	54.50+13.94	55.63+9.71

USPS and MINIST databases are shown in Table VIII, from which we can get the following observations:

- The kernel function $\kappa(\mathbf{x}_i, \mathbf{x}_j) = e^{-\frac{\|\mathbf{x}_i - \mathbf{x}_j\|^2}{\sigma^2}}$ achieves the best performance on USPS database. While the kernel function $\kappa(\mathbf{x}_i, \mathbf{x}_j) = (\mathbf{x}_i^T \mathbf{x}_j)^2$ obtains the best performance on MNIST database.
- The kernel function $\kappa(\mathbf{x}_i, \mathbf{x}_j) = (\mathbf{x}_i^T \mathbf{x}_j)^3$ outperforms $\kappa(\mathbf{x}_i, \mathbf{x}_j) = (\mathbf{x}_i^T \mathbf{x}_j)^2$ on USPS database, which is different to that on MNIST database. It is mainly caused by the fact that the images from USPS database lie in much higher nonlinear subspaces than that from MNIST database, and the former function induced a much more nonlinear mapping.
- The selection of different kernels results in a great

difference in the subspace clustering performance both on USPS database and MNIST database.

V. CONCLUSION

In this paper, we have incorporated the kernel technique into TRR method to achieve robust nonlinear subspace clustering. It does not need the prior knowledge about the structure of errors in the input data and remedies the drawback of the existing TRR method that it cannot deal with the data points from nonlinear subspaces. Moreover, through the theoretical analysis of our proposed mathematical model, we find that the developed optimization problem can be solved analytically, and the closed-form solution is only dependent on the kernel matrix. These advantages make our proposed method useful in many real-world applications. Comprehensive experiments

on four real-world image databases have demonstrated the effectiveness and the efficiency of the proposed method.

In the future, we plan to conduct a systematical investigation on the selection of optimal kernel for our proposed method and study how to determine the number of nonlinear subspaces automatically.

ACKNOWLEDGMENT

This work was supported in part by the National Natural Science Foundation of China under grants 61432012, 61329302, and the Engineering and Physical Sciences Research Council (EPSRC) of U.K. under grant EP/J017515/1.

REFERENCES

- [1] L. Parsons, E. Haque, and H. Liu, "Subspace clustering for high dimensional data: a review," *ACM SIGKDD Explorations Newsletter*, vol. 6, no. 1, pp. 90–105, 2004.
- [2] P. S. Bradley and O. L. Mangasarian, "k-plane clustering," *Journal of Global Optimization*, vol. 16, no. 1, pp. 23–32, 2000.
- [3] S. R. Rao, R. Tron, R. Vidal, and Y. Ma, "Motion segmentation via robust subspace separation in the presence of outlying, incomplete, or corrupted trajectories," in *Computer Vision and Pattern Recognition, 2008. CVPR 2008. IEEE Conference on*. IEEE, 2008, pp. 1–8.
- [4] H. Derksen, Y. Ma, W. Hong, and J. Wright, "Segmentation of multivariate mixed data via lossy coding and compression," *IEEE Transactions on Pattern Analysis and Machine Intelligence*, vol. 29, no. 9, p. 15461562, 2007.
- [5] J. P. Costeira and T. Kanade, "A multibody factorization method for independently moving objects," *International Journal of Computer Vision*, vol. 29, no. 3, pp. 159–179, 1998.
- [6] C. W. Gear, "Multibody grouping from motion images," *International Journal of Computer Vision*, vol. 29, no. 2, pp. 133–150, 1998.
- [7] R. Vidal, Y. Ma, and S. Sastry, "Generalized principal component analysis," *Pattern Analysis and Machine Intelligence, IEEE Transactions on*, vol. 27, no. 12, pp. 1945–1959, 2005.
- [8] A. Y. Ng, M. I. Jordan, and Y. Weiss, "On spectral clustering: Analysis and an algorithm," in *Advances in Neural Information Processing Systems*, vol. 14, 2002, Conference Proceedings, pp. 849–856.
- [9] U. Von Luxburg, "A tutorial on spectral clustering," *Statistics and Computing*, vol. 17, no. 4, pp. 395–416, 2007.
- [10] B. Cheng, J. Yang, S. Yan, Y. Fu, and T. S. Huang, "Learning with ℓ^1 -graph for image analysis," *IEEE Transactions on Image Processing*, vol. 19, no. 4, pp. 858–866, April 2010.
- [11] E. Elhamifar and R. Vidal, "Sparse subspace clustering: Algorithm, theory, and applications," *IEEE Transactions on Pattern Analysis and Machine Intelligence*, vol. 35, no. 11, pp. 2765–2781, 2013.
- [12] G. Liu, Z. Lin, S. Yan, J. Sun, Y. Yu, and Y. Ma, "Robust recovery of subspace structures by low-rank representation," *IEEE Transactions on Pattern Analysis and Machine Intelligence*, vol. 35, no. 1, pp. 171–184, 2013.
- [13] C. Y. Lu, H. Min, Z. Q. Zhao, L. Zhu, D. S. Huang, and S. C. Yan, "Robust and efficient subspace segmentation via least squares regression," in *Proc. of 12th Eur. Conf. Comput. Vis.*, Florence, Italy, Oct. 2012, pp. 347–360.
- [14] C. Lu, J. Tang, M. Lin, L. Lin, S. Yan, and Z. Lin, "Correntropy induced ℓ^2 graph for robust subspace clustering," in *2013 IEEE International Conference on Computer Vision*, Dec 2013, pp. 1801–1808.
- [15] V. M. Patel and R. Vidal, "Kernel sparse subspace clustering," in *Image Processing (ICIP), 2014 IEEE International Conference on*. IEEE, 2014, Conference Proceedings, pp. 2849–2853.
- [16] L. Zhen, Z. Yi, X. Peng, and D. Peng, "Locally linear representation for image clustering," *Electronics Letters*, vol. 50, no. 13, pp. 942–943, 2014.
- [17] X. Peng, Z. Yi, and H. Tang, "Robust subspace clustering via thresholding ridge regression," in *The Twenty-Ninth AAAI Conference on Artificial Intelligence*, 2015, Conference Proceedings, pp. 3827–3833.
- [18] H. Liu, T. Liu, J. Wu, D. Tao, and Y. Fu, "Spectral ensemble clustering," in *Proceedings of the 21th ACM SIGKDD International Conference on Knowledge Discovery and Data Mining*. ACM, 2015, pp. 715–724.
- [19] X. Peng, H. Tang, L. Zhang, Z. Yi, and S. Xiao, "A unified framework for representation-based subspace clustering of out-of-sample and large-scale data," *IEEE Transactions on Neural Networks and Learning Systems*, vol. 27, no. 12, pp. 2499–2512, Dec 2016.
- [20] X. Peng, C. Lu, Y. Zhang, and H. Tang, "Connections between nuclear norm and frobenius norm based representation," *IEEE Transactions on Neural Networks and Learning Systems*, vol. PP, no. 99, pp. 1–7, 2016.
- [21] E. Elhamifar and R. Vidal, "Sparse subspace clustering," in *IEEE Conference on Computer Vision and Pattern Recognition*, 2009, Conference Proceedings, pp. 2790–2797.
- [22] S. R. Rao, R. Tron, R. Vidal, and Y. Ma, "Motion segmentation via robust subspace separation in the presence of outlying, incomplete, or corrupted trajectories," in *Computer Vision and Pattern Recognition, 2008. CVPR 2008. IEEE Conference on*. IEEE, 2008, pp. 1–8.
- [23] Z. Yu, H.-S. Wong, and H. Wang, "Graph-based consensus clustering for class discovery from gene expression data," *Bioinformatics*, vol. 23, no. 21, pp. 2888–2896, 2007.
- [24] S. Xiao, M. Tan, D. Xu, and Z. Y. Dong, "Robust kernel low-rank representation," *IEEE Transactions on Neural Networks and Learning Systems*, 2015.
- [25] G. Liu and S. Yan, "Latent low-rank representation for subspace segmentation and feature extraction," in *2011 International Conference on Computer Vision*, Nov 2011, pp. 1615–1622.
- [26] E. Elhamifar and R. Vidal, "Sparse manifold clustering and embedding," in *Advances in Neural Information Processing Systems*, 2011, Conference Proceedings, pp. 55–63.
- [27] X. Peng, S. Xiao, J. Feng, W. Yau, and Z. Yi, "Deep subspace clustering with sparsity prior," in *Proceedings of the 25 International Joint Conference on Artificial Intelligence*, New York, NY, USA, 9–15 July 2016, pp. 1925–1931. [Online]. Available: <http://www.ijcai.org/Abstract/16/275>
- [28] X. Peng, J. Feng, J. Lu, W.-Y. Yau, and Z. Yi, "Cascade subspace clustering," in *Proceedings of the 31th AAAI Conference on Artificial Intelligence*. SFO, USA: AAAI, Feb. 2017, pp. 2478–2484.
- [29] J. Shawe-Taylor and N. Cristianini, *Kernel methods for pattern analysis*. Cambridge university press, 2004.
- [30] V. M. Patel and R. Vidal, "Kernel sparse subspace clustering," in *2014 IEEE International Conference on Image Processing (ICIP)*. IEEE, 2014, pp. 2849–2853.
- [31] K.-C. Lee, J. Ho, and D. J. Kriegman, "Acquiring linear subspaces for face recognition under variable lighting," *Pattern Analysis and Machine Intelligence, IEEE Transactions on*, vol. 27, no. 5, pp. 684–698, 2005.
- [32] S. K. N. S. A. Nene and H. Murase, "Columbia object image library (coil-20)," Report, 1996.
- [33] ———, "Columbia object image library (coil-100)," Report, 1996.
- [34] J. J. Hull, "A database for handwritten text recognition research," *Pattern Analysis and Machine Intelligence, IEEE Transactions on*, vol. 16, no. 5, pp. 550–554, 1994.
- [35] Y. LeCun, L. Bottou, Y. Bengio, and P. Haffner, "Gradient-based learning applied to document recognition," *Proceedings of the IEEE*, vol. 86, no. 11, pp. 2278–2324, 1998.
- [36] D. Cai, X. He, J. Han, and T. S. Huang, "Graph regularized nonnegative matrix factorization for data representation," *Pat-*

tern Analysis and Machine Intelligence, *IEEE Transactions on*, vol. 33, no. 8, pp. 1548–1560, 2011.

[37] J. Yan and M. Pollefeys, “A general framework for motion segmentation: Independent, articulated, rigid, non-rigid, degenerate and non-degenerate,” in *European conference on computer vision*. Springer, 2006, pp. 94–106.

[38] X. Zheng, D. Cai, X. He, W.-Y. Ma, and X. Lin, “Locality preserving clustering for image database,” in *Proceedings of the 12th annual ACM international conference on Multimedia*. ACM, Conference Proceedings, pp. 885–891.

[39] L. Hubert and P. Arabie, “Comparing partitions,” *Journal of classification*, vol. 2, no. 1, pp. 193–218, 1985.

[40] C. Goutte and E. Gaussier, *A probabilistic interpretation of precision, recall and F-score, with implication for evaluation*. Springer, 2005, pp. 345–359.

[41] J. D. Gibbons and S. Chakraborti, *Nonparametric statistical inference*. Springer, 2011.